Holographic Modeling and Realization of Topological Semimetal Coexistence States

Xuanting Ji

Collaboration with: Xiantong Chen, Haoqi Chu, Yan Liu, Ya-Wen Sun, Yun-Long Zhang

Based on: JHEP 12 (2021) 066
JHEP 05 (2024) 166
Eur. Phys. J. Plus 139, 485 (2024)
arXiv: 2501.XXXXX

China Agricultural University

December 3 2024

Outline

- Background
- Z_2 Weyl semimetal
- Effective field theory model of coexistence of topological semimetal
- Holographic coexistence of nodal line and Weyl semimetals
- Summary and outlook

Background

Condensed Matter Physics = Gravitational theory

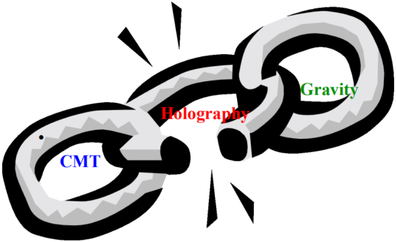

Background

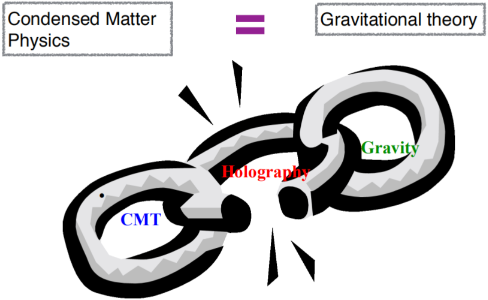

Superconductor, Mott insulator, Superfluid, Cold atoms, Strange metals, Topological states...

Background

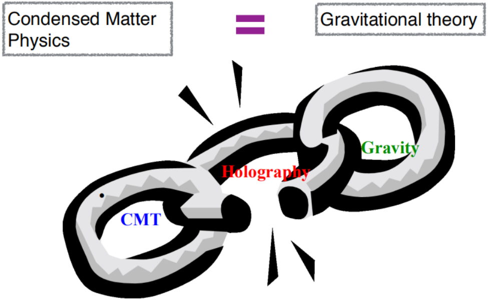

Superconductor, Mott insulator, Superfluid, Cold atoms, Strange metals, Topological states...

(quantum) Hall effect, Nernst effect, Anomoly induced transports...

Background

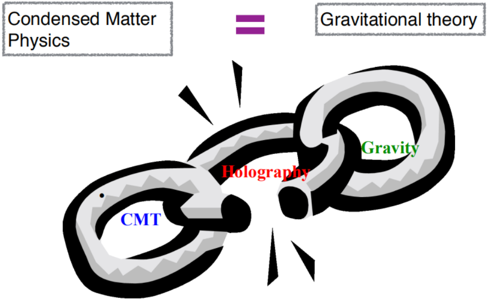

Superconductor, Mott insulator, Superfluid, Cold atoms, Strange metals, Topological states...
(quantum) Hall effect, Nernst effect, Anomoly induced transports...
SYK models...

- Beyond the Landau-Ginzburg paradigm;
- nontrivial topology in the quantum wave function;
- certain properties stable under small perturbations;
- (quantum)Topological phase transition.

Background

Topological semimetal family

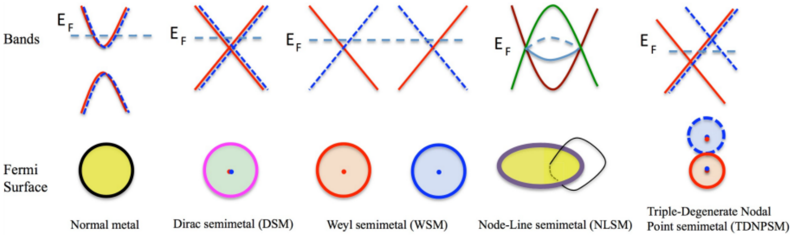

Classified according to the degeneracy and distribution in crystal momentum space.

H. Weng, X. Dai and Z. Fang, J. Phys.:Condens. Matter **28**, 303001 (2016)

H. Weng, Chin. Sci. Bull. (科学通报) 61, 3907-3916 (2016)

- Topological states of matter with strong interactions: difficulty in direct condensed matter calculations, especially for topological semimetals;
- Checking possible consequences of strong interactions: topological structure destroyed or new topological structures arise;
- New entry in the holographic dictionary: topological states of matter;
- Anomaly and anomalous transports;
- Holography;
- Topological phase transition.

Ideal Weyl semimetal

$$\mathcal{L}_{wsm} = \bar{\psi}\left(i\partial\!\!\!/ - eA\!\!\!/ - \gamma^{\mu}\gamma^{5}b_{\mu} + M\right)\psi\,,$$

where, $\bar{\psi} = \psi^{\dagger}\gamma^{0}$, γ^{μ} and γ^{5} are gamma matrices, b_{μ} is a time-reversal odd axial gauge field and M is the mass term.
D. Colladay and V. A. Kostelecky, Phys. Rev. D 58, 116002 (1998)

Background

Effective field theory model of topological semimetal

Ideal Weyl semimetal

$$\mathcal{L}_{wsm} = \bar{\psi}\left(i\partial\!\!\!/ - eA\!\!\!/ - \gamma^{\mu}\gamma^{5}b_{\mu} + M\right)\psi$$

where, $\bar{\psi} = \psi^{\dagger}\gamma^{0}$, γ^{μ} and γ^{5} are gamma matrices, b_{μ} is a time-reversal odd axial gauge field and M is the mass term.
D. Colladay and V. A. Kostelecky, Phys. Rev. D 58, 116002 (1998)

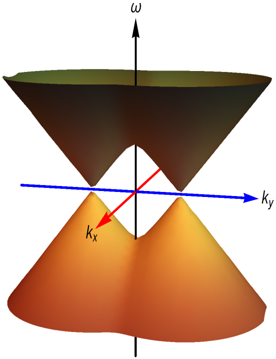

Background

Phase transition of the ideal Weyl semimetal

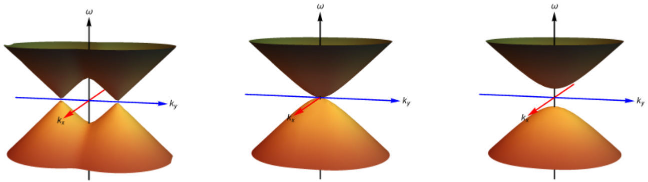

(a) Weyl semimetal phase (b) Critical point (c) Trivial phase

Background

Phase transition of the ideal Weyl semimetal

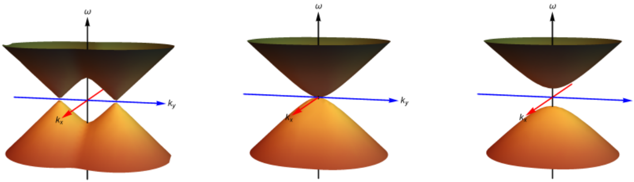

(a) Weyl semimetal phase (b) Critical point (c) Trivial phase

$|b| > |M|$ the spectrum is ungapped. The separation of the Weyl points in momentum space is given by $2b_{\text{eff}} = 2\sqrt{b^2 - M^2}$.
$|b| < |M|$ the system is gapped with gap $M_{\text{eff}} = \sqrt{M^2 - b^2}$.

Background

Phase transition of the ideal Weyl semimetal

The anomalous Hall effect $\overrightarrow{J} = \frac{1}{2\pi^2}\overrightarrow{b}_{eff} \times \overrightarrow{E}$ can be employed as an order parameter to indicate the occurrence of a phase transition.

Background

Phase transition of the ideal Weyl semimetal

The anomalous Hall effect $\overrightarrow{J} = \frac{1}{2\pi^2} \overrightarrow{b}_{eff} \times \overrightarrow{E}$ can be employed as an order parameter to indicate the occurrence of a phase transition. Topological invariants represent the intrinsic properties of the band structure, which can be defined for topological states of matter.

The anomalous Hall effect $\overrightarrow{J} = \frac{1}{2\pi^2}\overrightarrow{b}_{eff} \times \overrightarrow{E}$ can be employed as an order parameter to indicate the occurrence of a phase transition. Topological invariants represent the intrinsic properties of the band structure, which can be defined for topological states of matter. In a weakly coupled ideal Weyl semimetal, the corresponding topological invariant is defined as the Chern number. This is calculated by integrating the Berry curvature in the momentum space, and also can be calculated through the Green functions:

$$N(k_z) = \frac{1}{24\pi^2}\int dk_0 dk_x dk_y \mathrm{Tr}\left[\epsilon^{\mu\nu\rho z}\mathrm{G}\partial_\mu \mathrm{G}^{-1}\mathrm{G}\partial_\nu \mathrm{G}^{-1}\mathrm{G}\partial_\rho \mathrm{G}^{-1}\right],$$

(K. Ishikawa and T. Matsuyama, Z. Phys. C 33, 41(1986))

Background

Phase transition of the ideal Weyl semimetal

The topological number associated with each Weyl point is either +1 or -1, which correspond to opposite chiralities;
The merger of two Weyl points results in the formation of a Dirac point, characterised by a topological number of zero;
Upon the system becoming gapped, corresponds to the topological trivial phase, the topological number also reaches zero.

Background

Phase transition of the ideal Weyl semimetal

The topological number associated with each Weyl point is either +1 or -1, which correspond to opposite chiralities;
The merger of two Weyl points results in the formation of a Dirac point, characterised by a topological number of zero;
Upon the system becoming gapped, corresponds to the topological trivial phase, the topological number also reaches zero.

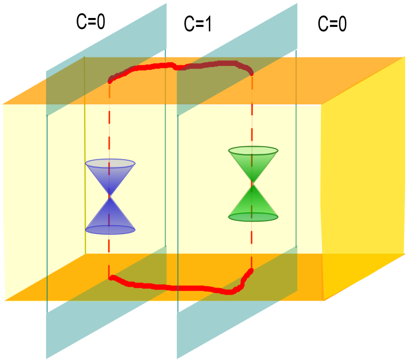

Nodal Line semimetal

$$\mathcal{L}_{nl} = \bar{\psi}\left(i\gamma^{\mu}\partial_{\mu} - M - \gamma^{\mu\nu}b_{\mu\nu}\right)\psi\,,$$

where, $\bar{\psi} = \psi^{\dagger}\gamma^{0}$,
$\gamma^{\mu\nu} = \frac{i}{2}[\gamma^{\mu}, \gamma^{\nu}]$, $b_{\mu\nu} = -b_{\nu\mu}$ is an external antisymmetric two-form field.
A. A. Burkov, M. D. Hook, L. Balents, Phys. Rev. B 84, 235126 (2011)

Nodal Line semimetal

$$\mathcal{L}_{nl} = \bar{\psi}(i\gamma^{\mu}\partial_{\mu} - M - \gamma^{\mu\nu}b_{\mu\nu})\psi \,,$$

where, $\bar{\psi} = \psi^{\dagger}\gamma^{0}$, $\gamma^{\mu\nu} = \frac{i}{2}[\gamma^{\mu}, \gamma^{\nu}]$, $b_{\mu\nu} = -b_{\nu\mu}$ is an external antisymmetric two-form field.
A. A. Burkov, M. D. Hook, L. Balents, Phys. Rev. B 84, 235126 (2011)

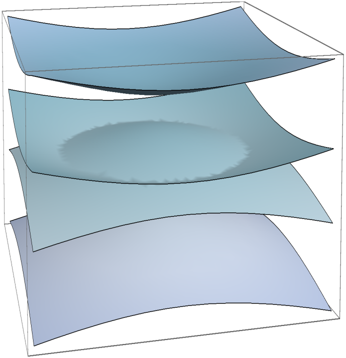

Model

- K. Landsteiner, Y. Liu, Phys. Lett. B **753**,453-457 (2016). (Ideal Weyl semimetal)
- Y. Liu and Y. W. Sun, JHEP **12**, 072 (2018). (Nodal line semimetal)
- V. Juricic, I. S. Landea, R. Soto-Garrido, JHEP **07**, 052 (2020). (Multi Weyl semimetal)
- **XTJ**, Yan Liu, Ya-Wen Sun, Yun-Long Zhang, JHEP **12**, 066 (2021). (Z_2 Weyl semimetal)
- K. Landsteiner, Y. Liu and Y. W. Sun, Sci. China Phys. Mech. Astron. **63**, 250001 (2020)....

Background

Holographic topological semimetals

Model

- K. Landsteiner, Y. Liu, Phys. Lett. B **753**,453-457 (2016). (Ideal Weyl semimetal)
- Y. Liu and Y. W. Sun, JHEP **12**, 072 (2018). (Nodal line semimetal)
- V. Juricic, I. S. Landea, R. Soto-Garrido, JHEP **07**, 052 (2020). (Multi Weyl semimetal)
- **XTJ**, Yan Liu, Ya-Wen Sun, Yun-Long Zhang, JHEP **12**, 066 (2021). (Z_2 Weyl semimetal)
- K. Landsteiner, Y. Liu and Y. W. Sun, Sci. China Phys. Mech. Astron. **63**, 250001 (2020)....

Transports

- K. Landsteiner, Y. Liu and Y. W. Sun, Phys. Rev. Lett., **117**, 081604(2016). (Odd viscosity)
- C. Copetti, J. Fernandez-Pendas, K. Landsteiner, JHEP **02**, 138(2017). (Axial Hall effect)
- G. Grignani, A. Marini, F. Pena-Benitez, S. Speziali, JHEP **03**, 125(2017). (AC conductivity)
- Y. Bu, R. G. Cai, Q. Yang, Y. L. Zhang, JHEP **09**, 083(2018). (chiral electric separation effect)
- **XTJ**, Y. Liu and X. M. Wu, Phys. Rev. D, **100**, 126013(2019). (chiral vortical conductivity)...

Background

Solid-liquid Coexistence State

Background

Solid-liquid Coexistence State

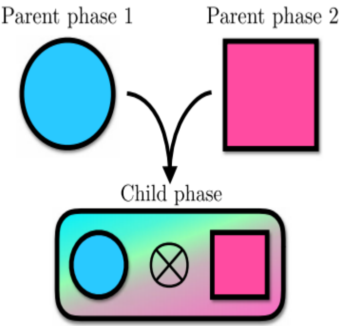

Multiplicative Topology

A. M. Cook, J. E. Moore, Commun Phys 5, 262 (2022)

Background

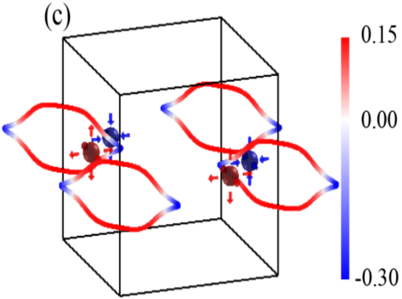

J. Zhan, J. Li, W. Shi, X. Chen, Y. Sun, Phys. Rev. B, 107: 224402(2023).

Background

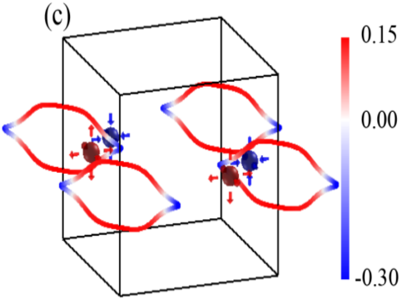

J. Zhan, J. Li, W. Shi, X. Chen, Y. Sun, Phys. Rev. B, 107: 224402(2023).

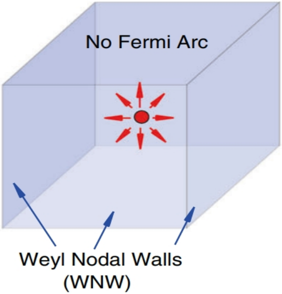

J.-Z. Ma, Q.-S. Wu, M. Song et al. Nat Commun 12, 3994 (2021).

Z_2 Weyl semimetal

Effective field theory model:

$$\mathcal{L}_{Z_2} = \Psi^\dagger \left[\Gamma^0 \left(i\Gamma^\mu \partial_\mu - e\Gamma^\mu A_\mu - \Gamma^\mu \Gamma^5 b_\mu + M_1 \mathbf{I}_1 + M_2 \mathbf{I}_2\right) + \hat{\Gamma}^0 \left(e\hat{\Gamma}^\mu \hat{A}_\mu - \hat{\Gamma}^\mu \hat{\Gamma}^5 c_\mu\right)\right] \Psi$$

Z_2 Weyl semimetal

Effective field theory model:

$$\mathcal{L}_{Z_2} = \Psi^\dagger \left[\Gamma^0 \left(i\Gamma^\mu \partial_\mu - e\Gamma^\mu A_\mu - \Gamma^\mu \Gamma^5 b_\mu + M_1 \mathbf{I}_1 + M_2 \mathbf{I}_2\right) + \hat{\Gamma}^0 \left(e\hat{\Gamma}^\mu \hat{A}_\mu - \hat{\Gamma}^\mu \hat{\Gamma}^5 c_\mu\right)\right] \Psi$$

- Ψ is an eight component spinor.
- $\Gamma^\mu \equiv \gamma^\mu \otimes \mathbb{I}_2\,, \quad \hat{\Gamma}^\mu \equiv \gamma^\mu \otimes \mathbb{Z}_2\,, \quad \Gamma^5 \equiv \gamma^5 \otimes \mathbb{I}_2\,, \quad \hat{\Gamma}^5 \equiv \gamma^5 \otimes \mathbb{Z}_2$, γ^μ is the 4×4 Dirac Gamma matrix.
- $\mathbb{I}_2 = \begin{pmatrix} 1 & 0 \\ 0 & 1 \end{pmatrix}, \mathbb{Z}_2 = \begin{pmatrix} 1 & 0 \\ 0 & -1 \end{pmatrix}$, $\mathbf{I}_1 = \text{diag}\,(1,0,1,0,1,0,1,0)$, $\mathbf{I}_2 = \text{diag}\,(0,1,0,1,0,1,0,1)$.
- b_μ is an axial gauge field, $\Gamma^\mu \Gamma^5 b_\mu$ is a Lorentz breaking term supporting the energy bands of the Weyl semimetal.

XTJ, Yan Liu, Ya-Wen Sun, Yun-Long Zhang, JHEP 12 (2021) 066.

Z_2 Weyl semimetal

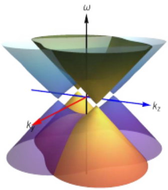

(a) Weyl-Z_2

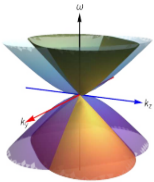

(b) double critical

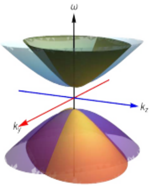

(c) gap-gap

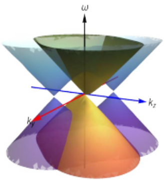

(d) Weyl/Z_2-critical

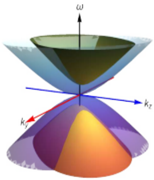

(e) critical-gap or gap-critical

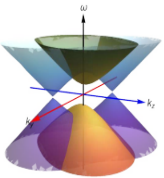

(f) Weyl/Z_2-gap

Z_2 Weyl semimetal

Holographic model:

$$
\begin{aligned}
S = \int d^5x\sqrt{-g}\bigg[&\frac{1}{2\kappa^2}\Big(R+\frac{12}{L^2}\Big)-\frac{1}{4}F^2-\frac{1}{4}\hat{F}^2-\frac{1}{4}F_5^2-\frac{1}{4}\hat{F}_5^2\\
&+\frac{\alpha}{3}\epsilon^{abcde}A_\mu^5\Big(F_{bc}^5F_{de}^5+3F_{bc}F_{de}+3\hat{F}_{bc}\hat{F}_{de}+\hat{F}_{bc}^5\hat{F}_{de}^5\Big)\\
&+\frac{2\beta}{3}\epsilon^{abcde}\hat{A}_\mu^5\Big(3\hat{F}_{bc}F_{de}+\hat{F}_{bc}^5F_{de}^5\Big)\\
&-(D^a\Phi_1)^*(D_a\Phi_1)-(\hat{D}^a\Phi_2)^*(\hat{D}_a\Phi_2)-V(\Phi_1,\Phi_2)\bigg]\,,
\end{aligned}
$$

Two Chern-Simons terms are responsible for the Chiral and Z_2 anomaly, respectively.

XTJ, Yan Liu, Ya-Wen Sun, Yun-Long Zhang, JHEP 12 (2021) 066.

Z_2 Weyl semimetal

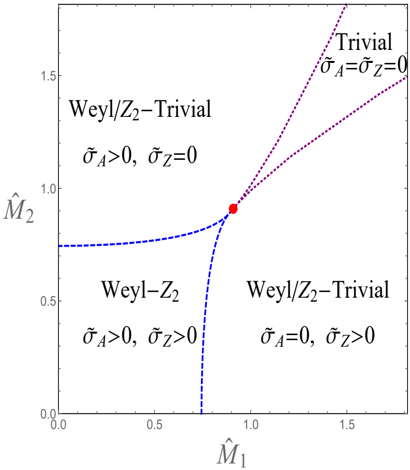

Z_2 Weyl semimetal

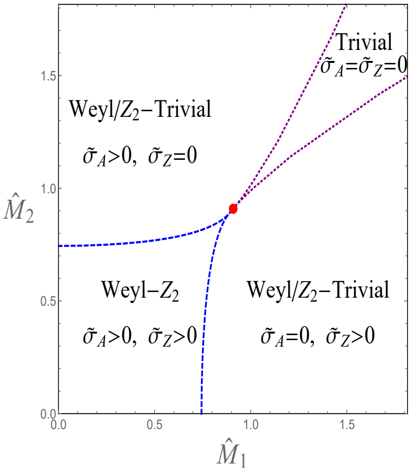

phase diagram in effective field theory model

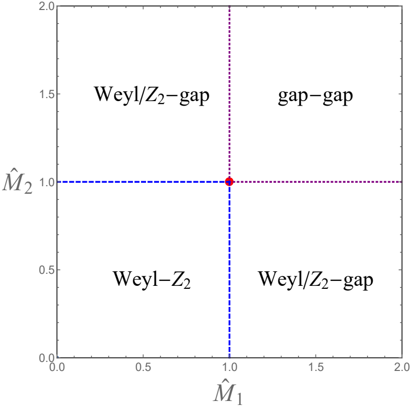

Z_2 Weyl semimetal

The determination of topological invariants from the Green function, $N(k_z) = \frac{1}{24\pi^2} \int dk_0 dk_x dk_y \mathrm{Tr}\left[\epsilon^{\mu\nu\rho z} \mathrm{G}\partial_\mu \mathrm{G}^{-1} \mathrm{G}\partial_\nu \mathrm{G}^{-1} \mathrm{G}\partial_\rho \mathrm{G}^{-1}\right]$, necessitates the utilisation of an integral in the $k_0 = i\omega$ direction.

Z_2 Weyl semimetal

The determination of topological invariants from the Green function, $N(k_z) = \frac{1}{24\pi^2} \int dk_0 dk_x dk_y \mathrm{Tr}\left[\epsilon^{\mu\nu\rho z} \mathrm{G}\partial_\mu \mathrm{G}^{-1} \mathrm{G}\partial_\nu \mathrm{G}^{-1} \mathrm{G}\partial_\rho \mathrm{G}^{-1}\right]$, necessitates the utilisation of an integral in the $k_0 = i\omega$ direction.

Topological invariants for interacting systems: the topological Hamiltonian method (Z. Wang and S.C. Zhang, Phys. Rev. X 2, 031008 (2012), Phys. Rev. X 4, 011006 (2014)):

The zero frequency Green function contains all topological information.

Topological Hamiltonian: $\mathcal{H}_t(\mathbf{k}) = -G^{-1}(0, \mathbf{k})$.

Z_2 Weyl semimetal

The determination of topological invariants from the Green function, $N(k_z) = \frac{1}{24\pi^2}\int dk_0 dk_x dk_y \mathrm{Tr}\left[\epsilon^{\mu\nu\rho z}\mathrm{G}\partial_\mu \mathrm{G}^{-1}\mathrm{G}\partial_\nu \mathrm{G}^{-1}\mathrm{G}\partial_\rho \mathrm{G}^{-1}\right]$, necessitates the utilisation of an integral in the $k_0 = i\omega$ direction.

Topological invariants for interacting systems: the topological Hamiltonian method (Z. Wang and S.C. Zhang, Phys. Rev. X 2, 031008 (2012), Phys. Rev. X 4, 011006 (2014)):

The zero frequency Green function contains all topological information.

Topological Hamiltonian: $\mathcal{H}_t(\mathbf{k}) = -G^{-1}(0, \mathbf{k})$.

For holographic model, one could detect the topological structure from the dual Green functions of probe fermions and calculate the topological invariants from the Green functions.

M. Cubrovic, J. Zaanen and K. Schalm, Science 325, 439 (2009),
H. Liu, J. McGreevy and D. Vegh, Phys. Rev. D 83, 065029 (2011),
Y. Liu and Y. W. Sun, JHEP 10 (2018) 189,
G. Song, J. Rong, S. J. Sin, JHEP 10 (2019) 109,
Y. Liu and X. M. Wu, JHEP 05 (2021) 141...

Z_2 Weyl semimetal

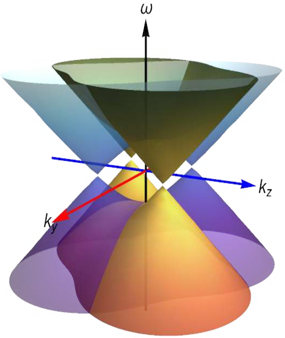

Z_2 Weyl semimetal

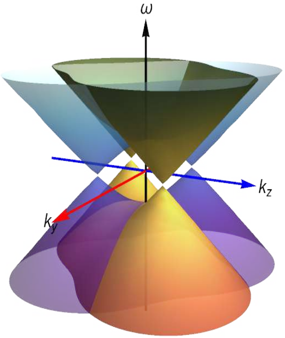

The system exhibits both chiral and Z_2 symmetry. The nodes are characterised by the topological charge $(\pm 1, \pm 1)$. The first ± 1 corresponds to the chiral symmetry, and the topological invariant is the chiral charge. The second ± 1 corresponds to the Z_2 symmetry, and the topological invariant is the Z_2 charge. Accordingly, two pairs of probe fermions are required to calculate the corresponding topological invariants in a Z_2 Weyl semimetal.

Z_2 Weyl semimetal

The probe fermion's action has the form like

$$S = S_1 + S_2 + S_3 + S_4 + S_\Phi$$

$$S_1 = \int \sqrt{-g} d^5x \bar{\Psi}_1 (\Gamma^a D_a - m_f) \Psi_1, \;\; S_2 = \int \sqrt{-g} d^5x \bar{\Psi}_2 (\Gamma^a D_a + m_f) \Psi_2$$

$$S_3 = \int \sqrt{-g} d^5x \bar{\Psi}_3 (\hat{\Gamma}^a \hat{D}_a - m_f) \Psi_3, \;\; S_4 = \int \sqrt{-g} d^5x \bar{\Psi}_4 (\hat{\Gamma}^a \hat{D}_a + m_f) \Psi_4$$

$$S_\Phi = - \int \sqrt{-g} d^5x (\eta_1 \Phi_1 \bar{\Psi}_1 \Psi_2 + \eta_1^* \Phi_1^* \bar{\Psi}_2 \Psi_1 + \eta_2 \Phi_2 \bar{\Psi}_3 \Psi_4 + \eta_2^* \Phi_2^* \bar{\Psi}_4 \Psi_3)$$

Where $\Gamma^a, D_a, \hat{\Gamma}^a, \hat{D}_a$ is defined as

$$\Gamma^a := \gamma^a \otimes \mathbb{I}_2, \;\; D_a := \nabla_a - i A_a$$

$$\hat{\Gamma}^a := \gamma^a \otimes \mathbb{Z}_2, \;\; \hat{D}_a := \nabla_a - i \hat{A}_a$$

Xiantong Chen, **XTJ** and Ya-Wen Sun, arXiv: 2501.XXXXX

Effective field theory model of coexistence of topological semimetal

$$\mathcal{L} = \Psi^\dagger \Gamma^0 \left[\left(i\Gamma^\mu \partial_\mu + \Gamma^{\mu\nu} b_{\mu\nu} + \Gamma^{\mu\nu}\Gamma^5 b^5_{\mu\nu} + M_1 \right) \mathbf{I}_1 + \left(i\Gamma^\mu \partial_\mu - \Gamma^0 \Gamma^\mu \Gamma^5 b_\mu + M_2 \right) \mathbf{I}_2 \right] \Psi,$$

Effective field theory model of coexistence of topological semimetal

$$\mathcal{L} = \Psi^\dagger \Gamma^0 \left[\left(i\Gamma^\mu \partial_\mu + \Gamma^{\mu\nu} b_{\mu\nu} + \Gamma^{\mu\nu}\Gamma^5 b^5_{\mu\nu} + M_1 \right) \mathbf{I}_1 + \left(i\Gamma^\mu \partial_\mu - \Gamma^0 \Gamma^\mu \Gamma^5 b_\mu + M_2 \right) \mathbf{I}_2 \right] \Psi,$$

- Ψ is an eight component spinor.
- $\Gamma^\mu \equiv \gamma^\mu \otimes \mathbb{I}_2\,, \quad \Gamma^5 \equiv \gamma^5 \otimes \mathbb{I}_2\,, \; \Gamma^{\mu\nu} = \frac{i}{2}[\Gamma^\mu, \Gamma^\nu]\,,\; \gamma^\mu$ is the 4×4 Dirac Gamma matrix and $\mathbb{I}_2$ is the 2×2 unit matrix.
- $\mathbf{I}_1 = \mathrm{diag}\,(1,0,1,0,1,0,1,0)$, $\mathbf{I}_2 = \mathrm{diag}\,(0,1,0,1,0,1,0,1)$.
- b_μ is an axial gauge field, $\Gamma^\mu\Gamma^5 b_\mu$ is a Lorentz breaking term supporting the energy bands of the Weyl semimetal.
- $b_{\mu\nu}$ is an antisymmetric real two-form field, and the term $\Gamma^{\mu\nu} b_{\mu\nu}$ contributes to the formation of the nodal line semimetal.
- $b^5_{\mu\nu}$ is a pure imaginary field, which is the dual part of the $b_{\mu\nu}$.

XTJ, Ya-Wen Sun, Eur. Phys. J. Plus 139, 485 (2024)

Effective field theory model of coexistence of topological semimetal

Set the non-zero component of the two-form field as b_{xy} in $\mathcal{L}$, then the non-zero component of the imaginary dual field $b^5_{\mu\nu}$ is $b^5_{tz} = ib_{xy}$. This choice results in a nodal ring in the $x - y$ plane.

To show the coexistence of the Weyl semimetal and the nodal semimetal intuitively, we will set b_x to be nonzero.

The energy spectrum of the eight eigenstates in $\mathcal{L}$ can be solved at the $k_z = 0$ plane as

$$\begin{aligned} E_{1n\pm} &= \pm\sqrt{\left(\sqrt{k_x^2 + k_y^2 + M_1^2} \mp 4b_{xy}\right)^2}, \\ E_{2w\pm} &= \pm\sqrt{\left(\sqrt{k_x^2 + M_2^2} \mp b_x\right)^2 + k_y^2}\,. \end{aligned}$$

Effective field theory model of coexistence of topological semimetal

Eight eigenstates above could be divided into two groups.

- $E_{1n\pm}$ is responsible for forming the nodal ring.
- $E_{2w\pm}$ is responsible for the Weyl nodes.
- Set $b_x = b\delta_x^\mu$ and $b_{xy} = c$.
- The effective radius of the nodal ring in the nodal line semimetal state is $\sqrt{16c^2 - M_1^2}$.
- The distance between two Weyl nodes is $\sqrt{b^2 - M_2^2}$.

Effective field theory model of coexistence of topological semimetal

Eight eigenstates above could be divided into two groups.

- $E_{1n\pm}$ is responsible for forming the nodal ring.
- $E_{2w\pm}$ is responsible for the Weyl nodes.
- Set $b_x = b\delta_x^\mu$ and $b_{xy} = c$.
- The effective radius of the nodal ring in the nodal line semimetal state is $\sqrt{16c^2 - M_1^2}$.
- The distance between two Weyl nodes is $\sqrt{b^2 - M_2^2}$.

Changing the values of M_1, M_2, b and c, different phases of the system can be found. The corresponding phase diagram can be drawn with three dimensionless parameters $\hat{M}_1 = M_1/c$, $\hat{M}_2 = M_2/b$ and c/b.

Effective field theory model of coexistence of topological semimetal

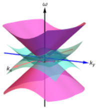

(a) Weyl-Nodal

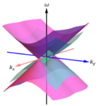

(b) Weyl-Critical

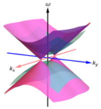

(c) Weyl-Gap

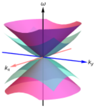

(d) Dirac Point(Critical)

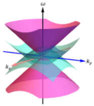

(e) Critical-Nodal

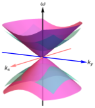

(f) Critical-Gap

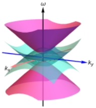

(g) Gap-Nodal

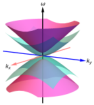

(h) Gap-Critical

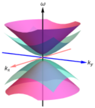

(i) Gap-Gap

Effective field theory model of coexistence of topological semimetal

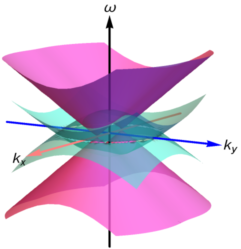

Weyl-nodal Coexistence State

Effective field theory model of coexistence of topological semimetal

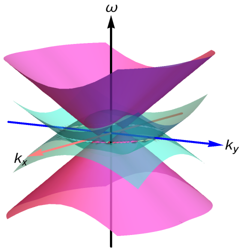

Weyl-nodal Coexistence State

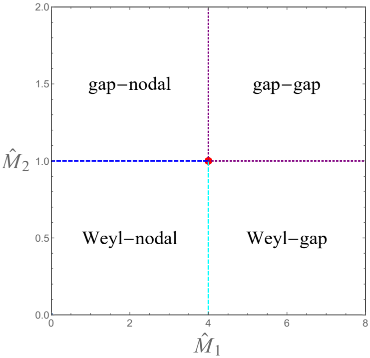

Phase diagram

Holographic coexistence of nodal line and Weyl semimetals

$$S = \int d^5x\sqrt{-g}\Big[\frac{1}{2\kappa^2}\Big(R+\frac{12}{L^2}\Big)-\frac{1}{4}\mathcal{F}^2-\frac{1}{4}\hat{\mathcal{F}}^2-\frac{1}{4}F_5^2-\frac{1}{4}\hat{F}_5^2$$
$$+\frac{\alpha}{3}\epsilon^{abcde}A_a\Big(3\mathcal{F}_{bc}\mathcal{F}_{de}+F^5_{bc}F^5_{de}+3\hat{\mathcal{F}}_{bc}\hat{\mathcal{F}}_{de}+\hat{F}^5_{bc}\hat{F}^5_{de}\Big)$$
$$+\frac{2\beta}{3}\epsilon^{abcde}\hat{A}_a\Big(3\hat{\mathcal{F}}_{bc}\mathcal{F}_{de}+\hat{F}^5_{bc}F^5_{de}\Big)-(\hat{D}^a\Phi_1)^*(\hat{D}_a\Phi_1)-(D^a\Phi_2)^*(D_a\Phi_2)$$
$$-\frac{1}{6\eta}\epsilon^{abcde}\Big(iB_{ab}H^*_{cde}-iB^*_{ab}H_{cde}\Big)-V_1(\Phi_1,\Phi_2)-V_2(B_{ab})-\lambda|\Phi_1|^2B^*_{ab}B^{ab}\Big],$$

κ^2 is the five dimensional gravitational constant, L is the AdS radius.
V and $\hat{V}$ are gauge fields represents the electromagnetic $U(1)$ current,
A_5 and $\hat{A}_5$ are the axial gauge field represents the axial $U(1)$ current.
B_{ab} is a complex anti-symmetric two form field, which is dual to operators $\bar{\psi}\gamma^{\mu\nu}\psi$ and $\bar{\psi}\gamma^{\mu\nu}\gamma^5\psi$ on the boundary.
Two scalar fields Φ_1 and Φ_2 denote the mass deformations.
Haoqi Chu, **XTJ**, Ya-Wen Sun, JHEP 05 (2024) 166

- the term proportional to α produces the chiral anomaly

$$\nabla_\mu J^\mu_5 = \lim_{r\to\infty}\Big[-\tfrac{\alpha}{3}\epsilon^{r\nu\rho\sigma\tau}\left(3F_{\nu\rho}F_{\sigma\tau}+F^5_{\nu\rho}F^5_{\sigma\tau}\right)-\tfrac{\beta}{3}\epsilon^{r\nu\rho\sigma\tau}\left(3\hat{F}_{\nu\rho}\hat{F}_{\sigma\tau}+\hat{F}^5_{\nu\rho}\hat{F}^5_{\sigma\tau}\right) - iq_1\left[\Phi_1^*(D^r\Phi_1)-\Phi_1(D^r\Phi_1)^*\right]\Big],$$

- the term proportional to β produces the Z_2 axial anomaly

$$\nabla_\mu \hat{J}^\mu_5 = \lim_{r\to\infty}\Big[-\tfrac{\alpha}{3}\epsilon^{r\nu\rho\sigma\tau}\left(3\hat{F}_{\nu\rho}F_{\sigma\tau}+F^5_{\nu\rho}\hat{F}^5_{\sigma\tau}\right)-\tfrac{\beta}{3}\epsilon^{r\nu\rho\sigma\tau}\left(3F_{\nu\rho}\hat{F}_{\sigma\tau}+\hat{F}^5_{\nu\rho}F^5_{\sigma\tau}\right) - iq_2\left[\Phi_2^*(\hat{D}^r\Phi_2)-\Phi_2(\hat{D}^r\Phi_2)^*\right]\Big].$$

- the term proportional to $\frac{1}{\eta}$ together with the mass term of the two-form field give rise to the equation of motion for the two-form field $B_{\mu\nu}$ with the self-duality relation of $B_{\mu\nu}$ taken into account.

Holographic coexistence of nodal line and Weyl semimetals

The Ansatz at zero temperature is

$$
\begin{aligned}
ds^2 &= -u(r)dt^2 + \frac{dr^2}{u(r)} + f(r)(dx^2 + dy^2) + h(r)dz^2\,,\\
\Phi_1 &= \phi_1(r)\,, \Phi_2 = \phi_2(r)\,,\\
A &= A_z(r)\,, B_{xy} = -B_{yx} = \mathcal{B}_{xy}\,, B_{tz} = -B_{zt} = i\mathcal{B}_{tz}\,,
\end{aligned}
$$

$u, f, h, A_z, \mathcal{B}_{xy}, \mathcal{B}_{tz}, \phi_1$ and ϕ_2 are functions of the radial coordinate r.

Holographic coexistence of nodal line and Weyl semimetals

The Ansatz at zero temperature is

$$
\begin{aligned}
ds^2 &= -u(r)dt^2 + \frac{dr^2}{u(r)} + f(r)(dx^2 + dy^2) + h(r)dz^2\,, \\
\Phi_1 &= \phi_1(r)\,, \Phi_2 = \phi_2(r)\,, \\
A &= A_z(r)\,, B_{xy} = -B_{yx} = \mathcal{B}_{xy}\,, B_{tz} = -B_{zt} = i\mathcal{B}_{tz}\,,
\end{aligned}
$$

$u, f, h, A_z, \mathcal{B}_{xy}, \mathcal{B}_{tz}, \phi_1$ and ϕ_2 are functions of the radial coordinate r.
The holographic analogues of the mass terms and the source term of the tensor operators are introduced in the UV boundary conditions

$$
\lim_{r\to\infty} r\Phi_1 = M_1\,, \quad \lim_{r\to\infty} r\Phi_2 = M_2\,,
$$

$$
\lim_{r\to\infty} A_z = b\,, \quad \lim_{r\to\infty} r^{-1}\mathcal{B}_{tz} = \lim_{r\to\infty} r^{-1}\mathcal{B}_{xy} = c.
$$

Holographic coexistence of nodal line and Weyl semimetals

- b: corresponds to the source of the chiral current $\Psi^\dagger\Gamma^0\Gamma^\mu\Gamma^5\Psi$.
- c: corresponds to the source of $\Psi^\dagger\Gamma^0\Gamma^{\mu\nu}\Psi$ as well as $\Psi^\dagger\Gamma^0\Gamma^{\mu\nu}\Gamma^5\Psi$.
- M_1 and M_2: sources of the $\Psi^\dagger\Gamma^0\mathbb{M}_1\Psi$ and $\Psi^\dagger\Gamma^0\mathbb{M}_2\Psi$, the mass terms of the fermions.

Holographic coexistence of nodal line and Weyl semimetals

- b: corresponds to the source of the chiral current $\Psi^\dagger\Gamma^0\Gamma^\mu\Gamma^5\Psi$.
- c: corresponds to the source of $\Psi^\dagger\Gamma^0\Gamma^{\mu\nu}\Psi$ as well as $\Psi^\dagger\Gamma^0\Gamma^{\mu\nu}\Gamma^5\Psi$.
- M_1 and M_2: sources of the $\Psi^\dagger\Gamma^0\mathbb{M}_1\Psi$ and $\Psi^\dagger\Gamma^0\mathbb{M}_2\Psi$, the mass terms of the fermions.

c and M_1 here should be responsible for the nodal line semimetal, i.e. a certain combination of them determines the effective radius of the nodal ring. Similarly, the boundary values of b and M_2 are responsible for the Weyl nodes, and a combination of them shows the effective distance between the two Weyl nodes.

Holographic coexistence of nodal line and Weyl semimetals

- b: corresponds to the source of the chiral current $\Psi^\dagger\Gamma^0\Gamma^\mu\Gamma^5\Psi$.
- c: corresponds to the source of $\Psi^\dagger\Gamma^0\Gamma^{\mu\nu}\Psi$ as well as $\Psi^\dagger\Gamma^0\Gamma^{\mu\nu}\Gamma^5\Psi$.
- M_1 and M_2: sources of the $\Psi^\dagger\Gamma^0\mathbb{M}_1\Psi$ and $\Psi^\dagger\Gamma^0\mathbb{M}_2\Psi$, the mass terms of the fermions.

c and M_1 here should be responsible for the nodal line semimetal, i.e. a certain combination of them determines the effective radius of the nodal ring. Similarly, the boundary values of b and M_2 are responsible for the Weyl nodes, and a combination of them shows the effective distance between the two Weyl nodes. Nine different types of IR solutions can be found, which flow to the asymptotic AdS_5 boundary to give nine types of full spacetime solutions. From the IR behavior of these nine solutions and the boundary value of each IR solution, a phase diagram similar to the weakly coupled one can be obtained.

Holographic coexistence of nodal line and Weyl semimetals

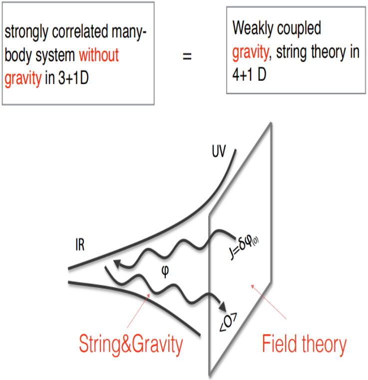

Holographic coexistence of nodal line and Weyl semimetals

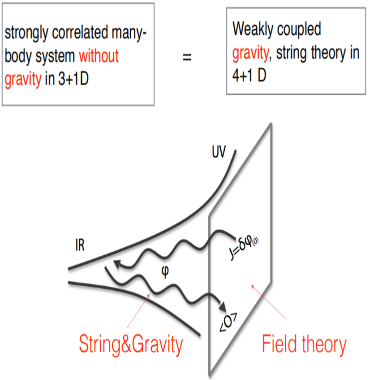

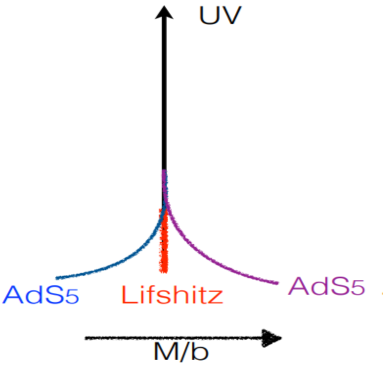

Double Critical Point

$$
ds^2 = u_0 r^2 \left(-dt^2 + dx^2\right) + \frac{dr^2}{u_0 r^2}
$$

$$
+ f_0 r^\alpha dy^2 + h_0 r^{2\alpha_1} dz^2 \,,
$$

$$
A_z = r^{\alpha_1} \,, \quad \phi_1 = \phi_{10} \,, \quad \phi_2 = \phi_{20} \,,
$$

$$
\mathcal{B}_{xy} = b_{xy}^{(c)} r^\alpha \,, \quad \mathcal{B}_{tz} = b_{tz}^{(c)} r^{1+\alpha_1} \,,
$$

with $c/b = 1$,
$\hat{M}_1 \equiv \frac{M_1}{c} = 1.073$,
$\hat{M}_2 \equiv \frac{M_2}{b} = 0.924$.

Double Critical Point

$$ds^2 = u_0 r^2 \left(-dt^2 + dx^2\right) + \frac{dr^2}{u_0 r^2}$$
$$+ f_0 r^\alpha dy^2 + h_0 r^{2\alpha_1} dz^2 \,,$$
$$A_z = r^{\alpha_1} \,, \quad \phi_1 = \phi_{10} \,, \quad \phi_2 = \phi_{20} \,,$$
$$\mathcal{B}_{xy} = b_{xy}^{(c)} r^\alpha \,, \quad \mathcal{B}_{tz} = b_{tz}^{(c)} r^{1+\alpha_1} \,,$$

with $c/b = 1$,
$\hat{M}_1 \equiv \frac{M_1}{c} = 1.073$,
$\hat{M}_2 \equiv \frac{M_2}{b} = 0.924$.

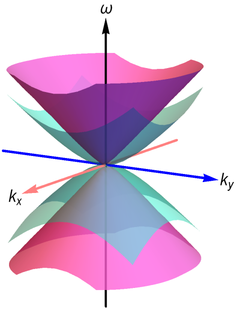

Weyl-Critical

$$
\begin{aligned}
u &= u_0\, r^2 \left(1 + \delta u_1\, r^{\alpha_1}\right) \,, \\
f &= f_0\, r^{2\alpha} \left(1 + \delta f_1\, r^{\alpha_1}\right) \,, \\
h &= h_0\, r^2 \left(1 + \delta h_1\, r^{\alpha_1}\right) \,, \\
A_z &= a_0 + \phi_{20}^2 r^{1-\alpha} h_0 \exp\left(-\frac{3a_0}{r\sqrt{u_0 h_0}}\right) \,, \\
\mathcal{B}_{tz} &= b_{tz0} r^2 \left(1 + \delta \mathcal{B}_{tz1}\, r^{\alpha_1}\right) \,, \\
\mathcal{B}_{xy} &= r^{\alpha} \left(1 + \delta \mathcal{B}_{xy1}\, r^{\alpha_1}\right) \,, \\
\Phi_1 &= \phi_{10} \left(1 + \delta \phi_{11}\, r^{\alpha_1}\right) \,, \\
\Phi_2 &= \phi_{20} \exp\left(-\frac{3a_0}{2r\sqrt{u_0 h_0}}\right) r^{\frac{-1-\alpha}{2}} \,.
\end{aligned}
$$

Weyl-Critical

$$
\begin{aligned}
u &= u_0\, r^2 \left(1 + \delta u_1\, r^{\alpha_1}\right) \,, \\
f &= f_0\, r^{2\alpha} \left(1 + \delta f_1\, r^{\alpha_1}\right) \,, \\
h &= h_0\, r^2 \left(1 + \delta h_1\, r^{\alpha_1}\right) \,, \\
A_z &= a_0 + \phi_{20}^2 r^{1-\alpha} h_0 \exp\left(-\frac{3a_0}{r\sqrt{u_0 h_0}}\right) \\
\mathcal{B}_{tz} &= b_{tz0} r^2 \left(1 + \delta\mathcal{B}_{tz1}\, r^{\alpha_1}\right) \,, \\
\mathcal{B}_{xy} &= r^{\alpha} \left(1 + \delta\mathcal{B}_{xy1}\, r^{\alpha_1}\right) \,, \\
\Phi_1 &= \phi_{10} \left(1 + \delta\phi_{11}\, r^{\alpha_1}\right) \,, \\
\Phi_2 &= \phi_{20} \exp\left(-\frac{3a_0}{2r\sqrt{u_0 h_0}}\right) r^{\frac{-1-\alpha}{2}} \,.
\end{aligned}
$$

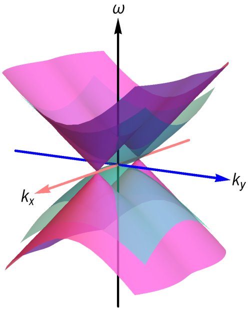

Critical-Nodal

$$
\begin{aligned}
u &= u_0\, r^2 \left(1 + \delta u_1\, r^{\alpha_1}\right) \ , \\
f &= f_0\, r^{2\alpha} \left(1 + \delta f_1\, r^{\alpha_1}\right) \ , \\
h &= h_0\, r^{2\alpha_2} \left(1 + \delta h_1\, r^{\alpha_1}\right) \ , \\
A_z &= r^{\alpha_2} \left(1 + \delta a_1\, r^{\alpha_1}\right) \ , \\
\mathcal{B}_{tz} &= b_{tz0} r^{1+\alpha_2} \left(1 + \delta \mathcal{B}_{tz1}\, r^{\alpha_1}\right) \ , \\
\mathcal{B}_{xy} &= r^{\alpha} \left(1 + \delta \mathcal{B}_{xy1}\, r^{\alpha_1}\right) \ , \\
\Phi_1 &= \phi_{10} r^{\beta} \, , \\
\Phi_2 &= \phi_{20} \left(1 + \delta \phi_{21}\, r^{\alpha_1}\right) \ .
\end{aligned}
$$

Critical-Nodal

$$u = u_0\, r^2 \left(1 + \delta u_1\, r^{\alpha_1}\right) \ ,$$
$$f = f_0\, r^{2\alpha} \left(1 + \delta f_1\, r^{\alpha_1}\right) \ ,$$
$$h = h_0\, r^{2\alpha_2} \left(1 + \delta h_1\, r^{\alpha_1}\right) \ ,$$
$$A_z = r^{\alpha_2} \left(1 + \delta a_1\, r^{\alpha_1}\right) \ ,$$
$$\mathcal{B}_{tz} = b_{tz0} r^{1+\alpha_2} \left(1 + \delta \mathcal{B}_{tz1}\, r^{\alpha_1}\right) \ ,$$
$$\mathcal{B}_{xy} = r^{\alpha} \left(1 + \delta \mathcal{B}_{xy1}\, r^{\alpha_1}\right) \ ,$$
$$\Phi_1 = \phi_{10} r^{\beta} \, ,$$
$$\Phi_2 = \phi_{20} \left(1 + \delta \phi_{21}\, r^{\alpha_1}\right) \ .$$

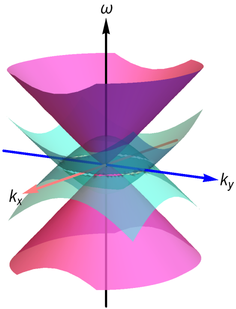

Critical-Gap

$$
\begin{aligned}
u &= u_0\, r^2 \left(1 + \delta u_1\, r^{\alpha_1}\right) , \\
f &= r^2 \left(1 + \delta f_1\, r^{\alpha_1}\right) , \\
h &= h_0\, r^{2\alpha} \left(1 + \delta h_1\, r^{\alpha_1}\right) , \\
A_z &= r^{\alpha} \left(1 + \delta a_1\, r^{\alpha_1}\right) , \\
\mathcal{B}_{tz} &= \mathcal{B}_{tz0} r^{\alpha_2} , \\
\mathcal{B}_{xy} &= \mathcal{B}_{xy0} r^{\alpha_2} , \\
\Phi_1 &= \sqrt{30} \left(1 + \delta\phi_{11}\, r^{\beta}\right) , \\
\Phi_2 &= \phi_{20} \left(1 + \delta\phi_{21} r^{\alpha_1}\right) .
\end{aligned}
$$

Critical-Gap

$$
\begin{aligned}
u &= u_0\, r^2 \left(1 + \delta u_1\, r^{\alpha_1}\right) \,, \\
f &= r^2 \left(1 + \delta f_1\, r^{\alpha_1}\right) \,, \\
h &= h_0\, r^{2\alpha} \left(1 + \delta h_1\, r^{\alpha_1}\right) \,, \\
A_z &= r^{\alpha} \left(1 + \delta a_1\, r^{\alpha_1}\right) \,, \\
\mathcal{B}_{tz} &= \mathcal{B}_{tz0} r^{\alpha_2} \,, \\
\mathcal{B}_{xy} &= \mathcal{B}_{xy0} r^{\alpha_2} \,, \\
\Phi_1 &= \sqrt{30} \left(1 + \delta\phi_{11}\, r^{\beta}\right) \,, \\
\Phi_2 &= \phi_{20} \left(1 + \delta\phi_{21} r^{\alpha_1}\right) \,.
\end{aligned}
$$

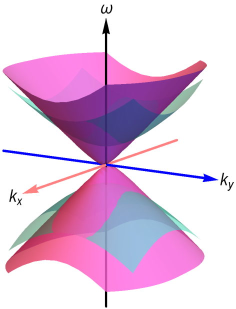

Gap-Critical

$$
\begin{aligned}
u &= u_0\, r^2 \left(1+\delta u_1\, r^{\alpha_1} + \delta u_2\, r^{2\alpha_3-2}\right) ,\\
f &= f_0\, r^{\alpha} \left(1+\delta f_1\, r^{\alpha_1} + \delta f_2\, r^{2\alpha_3-2}\right) ,\\
h &= u_0\, r^2 \left(1+\delta h_1\, r^{\alpha_1} + \delta h_2\, r^{2\alpha_3-2}\right) ,\\
A_z &= a_0\, r^{\alpha_3} ,\\
\mathcal{B}_{tz} &= \mathcal{B}_{tz0} r^2 \left(1+\delta \mathcal{B}_{tz1}\, r^{\alpha_1} + \delta \mathcal{B}_{tz2}\, r^{2\alpha_3-2}\right) ,\\
\mathcal{B}_{xy} &= \mathcal{B}_{xy0} r^{\alpha} \left(1+\delta \mathcal{B}_{xy1}\, r^{\alpha_1} + \delta \mathcal{B}_{xy2}\, r^{2\alpha_3-2}\right) ,\\
\Phi_1 &= \phi_{10} \left(1+\delta \phi_{11}\, r^{\alpha_1} + \delta \phi_{12}\, r^{2\alpha_3-2}\right) ,\\
\Phi_2 &= \sqrt{30} \left(1+\delta\phi_{21} r^{\alpha_2} + r^{\frac{1}{2}\left(-\alpha+\frac{\sqrt{(\alpha+2)^2 \mathrm{u0}+24}}{\sqrt{\mathrm{u0}}}-2\right)}\right) .
\end{aligned}
$$

Gap-Critical

$$u = u_0\, r^2 \left(1 + \delta u_1\, r^{\alpha_1} + \delta u_2\, r^{2\alpha_3 - 2}\right) ,$$
$$f = f_0\, r^{\alpha} \left(1 + \delta f_1\, r^{\alpha_1} + \delta f_2\, r^{2\alpha_3 - 2}\right) ,$$
$$h = u_0\, r^2 \left(1 + \delta h_1\, r^{\alpha_1} + \delta h_2\, r^{2\alpha_3 - 2}\right) ,$$
$$A_z = a_0\, r^{\alpha_3} ,$$
$$\mathcal{B}_{tz} = \mathcal{B}_{tz0} r^2 \left(1 + \delta\mathcal{B}_{tz1}\, r^{\alpha_1} + \delta\mathcal{B}_{tz2}\, r^{2\alpha_3 - 2}\right) ,$$
$$\mathcal{B}_{xy} = \mathcal{B}_{xy0} r^{\alpha} \left(1 + \delta\mathcal{B}_{xy1}\, r^{\alpha_1} + \delta\mathcal{B}_{xy2}\, r^{2\alpha_3 - 2}\right.$$
$$\Phi_1 = \phi_{10} \left(1 + \delta\phi_{11}\, r^{\alpha_1} + \delta\phi_{12}\, r^{2\alpha_3 - 2}\right) ,$$
$$\Phi_2 = \sqrt{30} \left(1 + \delta\phi_{21} r^{\alpha_2} + r^{\frac{1}{2}\left(-\alpha + \frac{\sqrt{(\alpha+2)^2 \mathrm{u0} +}}{\sqrt{\mathrm{u0}}}\right.}\right.$$

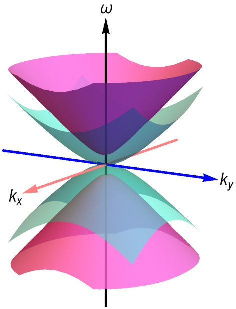

Weyl-Nodal

$$
\begin{aligned}
u &= u_0\, r^2 \left(1 + \delta u\, r^{\alpha_1}\right) \,, \\
f &= f_0\, r^{\alpha} \left(1 + \delta f\, r^{\alpha_1}\right) \,, \\
h &= r^2 \left(1 + \delta h\, r^{\alpha_1}\right) \,, \\
A_z &= a_0 + \exp\left(-\frac{3a_0}{r\sqrt{u_0}}\right) r^{\alpha-1} \,, \\
\mathcal{B}_{tz} &= \mathcal{B}_{tz0} r^2 \left(1 + \delta\mathcal{B}_{tz}\, r^{\alpha_1}\right) \,, \\
\mathcal{B}_{xy} &= r^{\alpha} \left(1 + \delta\mathcal{B}_{xy}\, r^{\alpha_1}\right) \,, \\
\Phi_1 &= \phi_{10}\, r^{\beta} \,, \\
\Phi_2 &= \phi_{20} \exp\left(-\frac{3a_0}{2r\sqrt{u_0}}\right) r^{-\frac{1+\alpha}{2}} \,.
\end{aligned}
$$

Weyl-Nodal

$$u = u_0\, r^2 \left(1 + \delta u\, r^{\alpha_1}\right) \,,$$
$$f = f_0\, r^{\alpha} \left(1 + \delta f\, r^{\alpha_1}\right) \,,$$
$$h = r^2 \left(1 + \delta h\, r^{\alpha_1}\right) \,,$$
$$A_z = a_0 + \exp\left(-\frac{3a_0}{r\sqrt{u_0}}\right) r^{\alpha-1} \,,$$
$$\mathcal{B}_{tz} = \mathcal{B}_{tz0} r^2 \left(1 + \delta\mathcal{B}_{tz}\, r^{\alpha_1}\right) \,,$$
$$\mathcal{B}_{xy} = r^{\alpha} \left(1 + \delta\mathcal{B}_{xy}\, r^{\alpha_1}\right) \,,$$
$$\Phi_1 = \phi_{10}\, r^{\beta} \,,$$
$$\Phi_2 = \phi_{20} \exp\left(-\frac{3a_0}{2r\sqrt{u_0}}\right) r^{-\frac{1+\alpha}{2}} \,.$$

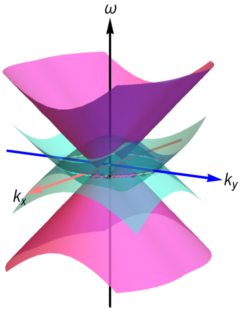

Weyl-Gap

$$
\begin{aligned}
u &= u_0\, r^2\,, \\
f &= h = r^2\,, \\
A_z &= a_0 + \exp\left(-\frac{3a_0}{r\sqrt{u_0}}\right)\left(\frac{\phi_{20}^2 u_0}{9\pi a_0^3} + \frac{\phi_{20}^2\sqrt{u_0}}{3\pi a_0^2 r}\right)\,, \\
\mathcal{B}_{tz} &= \mathcal{B}_{tz0} r^{\beta}\,, \\
\mathcal{B}_{xy} &= \mathcal{B}_{xy0} r^{\beta}\,, \\
\Phi_1 &= \phi_{10} + \phi_{11}\, r^{\alpha}\,, \\
\Phi_2 &= 2\phi_{20}\frac{\exp\left(-\frac{3a_0}{2r\sqrt{u_0}}\right)}{\sqrt{3\pi}r^2\sqrt{\frac{a_0}{r\sqrt{u_0}}}}\,.
\end{aligned}
$$

Holographic coexistence of nodal line and Weyl semimetals

Weyl-Gap

$$u = u_0\, r^2\,,$$
$$f = h = r^2\,,$$
$$A_z = a_0 + \exp\left(-\frac{3a_0}{r\sqrt{u_0}}\right)\left(\frac{\phi_{20}^2 u_0}{9\pi a_0^3} + \frac{\phi_{2}^2}{3}\right.$$
$$\mathcal{B}_{tz} = \mathcal{B}_{tz0} r^{\beta}\,,$$
$$\mathcal{B}_{xy} = \mathcal{B}_{xy0} r^{\beta}\,,$$
$$\Phi_1 = \phi_{10} + \phi_{11}\, r^{\alpha}\,,$$
$$\Phi_2 = 2\phi_{20}\frac{\exp\left(-\frac{3a_0}{2r\sqrt{u_0}}\right)}{\sqrt{3\pi}r^2\sqrt{\frac{a_0}{r\sqrt{u_0}}}}\,.$$

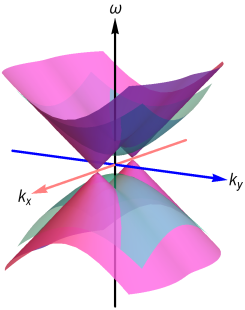

Gap-Nodal

$$
\begin{aligned}
u &= u_0\, r^2 \left(1 + \delta u_1\, r^{\alpha_1}\right) , \\
f &= f_0\, r^{\alpha} \left(1 + \delta f_1\, r^{\alpha_1}\right) , \\
h &= r^2 \left(1 + \delta h_1\, r^{\alpha_1}\right) , \\
A_z &= a_0 r^{\alpha_2} , \\
\mathcal{B}_{tz} &= b_{tz0} r^2 \left(1 + \delta \mathcal{B}_{tz1}\, r^{\alpha_1}\right) , \\
\mathcal{B}_{xy} &= r^{\alpha} \left(1 + \delta \mathcal{B}_{xy1}\, r^{\alpha_1}\right) , \\
\Phi_1 &= \phi_{10} r^{\beta} , \\
\Phi_2 &= \phi_{20} + \phi_{21}\, r^{\alpha_3} .
\end{aligned}
$$

Gap-Nodal

$$u = u_0\, r^2\, (1 + \delta u_1\, r^{\alpha_1})\ ,$$
$$f = f_0\, r^{\alpha}\, (1 + \delta f_1\, r^{\alpha_1})\ ,$$
$$h = r^2\, (1 + \delta h_1\, r^{\alpha_1})\ ,$$
$$A_z = a_0 r^{\alpha_2}\ ,$$
$$\mathcal{B}_{tz} = b_{tz0} r^2\, (1 + \delta\mathcal{B}_{tz1}\, r^{\alpha_1})\ ,$$
$$\mathcal{B}_{xy} = r^{\alpha}\, (1 + \delta\mathcal{B}_{xy1}\, r^{\alpha_1})\ ,$$
$$\Phi_1 = \phi_{10} r^{\beta}\ ,$$
$$\Phi_2 = \phi_{20} + \phi_{21}\, r^{\alpha_3}\ .$$

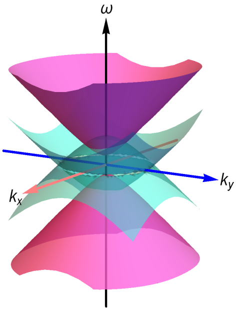

Gap-Gap

$$
\begin{aligned}
&u = u_0\, r^2\,,\\
&f = h = r^2\,,\\
&A_z = a_0 r^{\alpha_1},\\
&\mathcal{B}_{tz} = \mathcal{B}_{tz0} r^{\beta}\,,\\
&\mathcal{B}_{xy} = \mathcal{B}_{xy0} r^{\beta}\,,\\
&\Phi_1 = \phi_{10} + \phi_{11}\, r^{\alpha_2}\,,\\
&\Phi_2 = \phi_{20} + \phi_{21}\, r^{\alpha_2}\,.
\end{aligned}
$$

Gap-Gap

$$
\begin{aligned}
u &= u_0\, r^2\,, \\
f &= h = r^2\,, \\
A_z &= a_0 r^{\alpha_1}, \\
\mathcal{B}_{tz} &= \mathcal{B}_{tz0} r^{\beta}\,, \\
\mathcal{B}_{xy} &= \mathcal{B}_{xy0} r^{\beta}\,, \\
\Phi_1 &= \phi_{10} + \phi_{11}\, r^{\alpha_2}\,, \\
\Phi_2 &= \phi_{20} + \phi_{21}\, r^{\alpha_2}\,.
\end{aligned}
$$

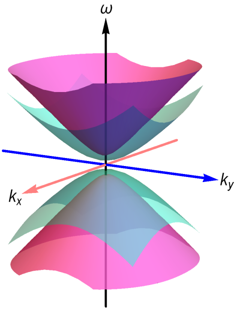

Holographic coexistence of nodal line and Weyl semimetals

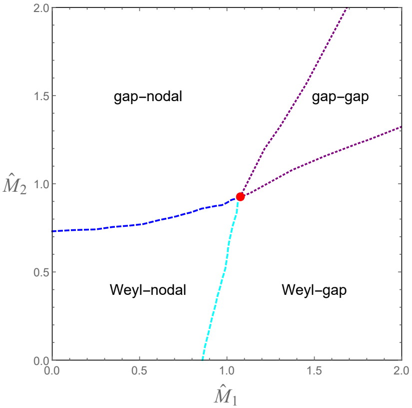

Holographic coexistence of nodal line and Weyl semimetals

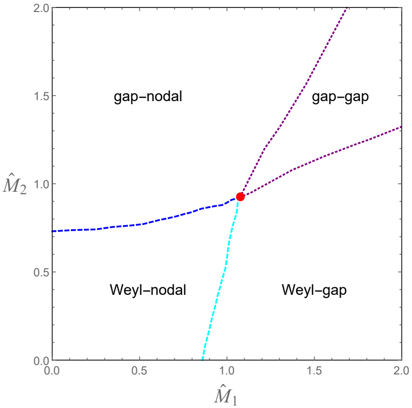

phase diagram in effective field theory model

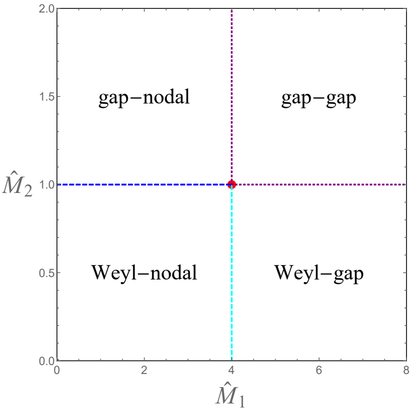

anomalous Hall conductivity

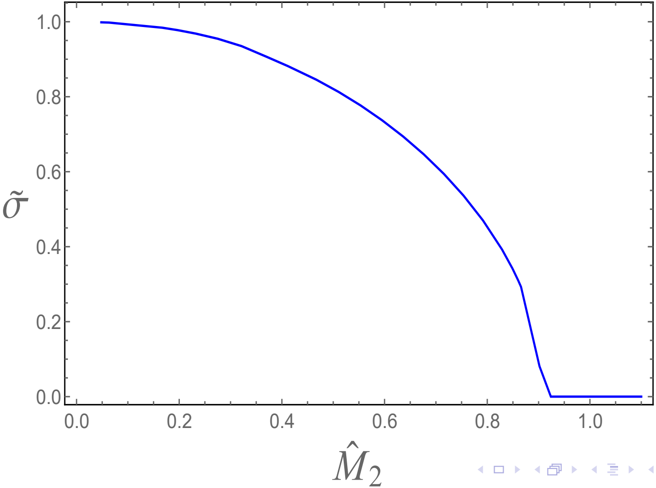

free energy

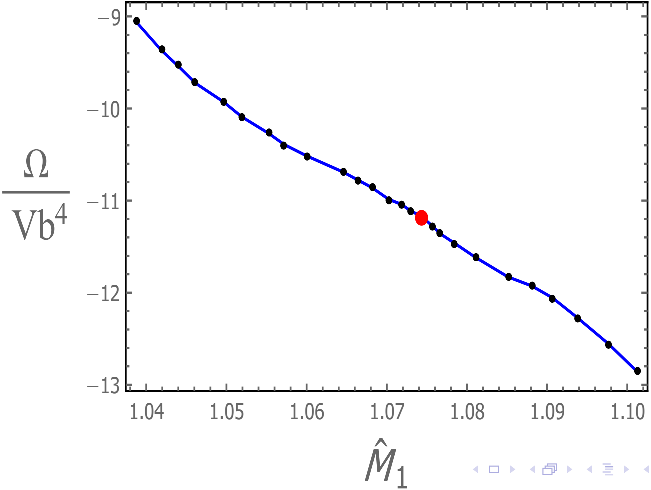

Summary and outlook

Summary

- Construct holographic models that allows for the coexistence of the ideal Weyl semimetal and the nodal line semimetal
- Similar phase diagram with the weak coupling regime
- Anomalous Hall conductivity, free energy to demonstrate the continuation of the phase transition.

Outlook

- How to realize the triple degenerate nodal point phase by holographic model?
- Calculate the topological invariants of the system, to ascertain whether there are any finite temperature effects.
- Gain a deeper comprehension of the disorder effect in condensed matter systems through holography.


Thanks!
天涯